

On the compatibility of a flux transport dynamo with a fast tachocline scenario

Bidya Binay Karak¹ · Kristof Petrovay²

© Springer ●●●●

Abstract The compatibility of the fast tachocline scenario with a flux transport dynamo model is explored. We employ a flux transport dynamo model coupled with simple feedback formulae relating the thickness of the tachocline to the amplitude of the magnetic field or to the Maxwell stress. The dynamo model is found to be robust against the nonlinearity introduced by this simplified fast tachocline mechanism. Solar-like butterfly diagrams are found to persist and, even without any parameter fitting, the overall thickness of the tachocline is well within the range admitted by helioseismic constraints. In the most realistic case of a time and latitude dependent tachocline thickness linked to the value of the Maxwell stress, both the thickness and its latitude dependence are in excellent agreement with seismic results. In the nonparametric models, cycle related temporal variations in tachocline thickness are somewhat larger than admitted by helioseismic constraints; we find, however, that introducing a further parameter into our feedback formula readily allows further fine tuning of the thickness variations.

Keywords: dynamo, tachocline

1. Introduction

Flux transport dynamos are the most widely discussed scenario for the origin of solar activity. In these models, the α -effect responsible for toroidal \rightarrow poloidal flux conversion is identified with the tilting of the axis of active regions relative to the azimuthal direction. The poloidal field generated by this α -effect concentrated near the surface is then transported by the meridional circulation to high latitudes and then down to the bottom of the convective zone (Babcock–Leighton mechanism). The return branch of a one-celled circulation flow pattern will then advect the field back towards the equator while differential rotation amplifies it to a toroidal field of increasing strength (Ω -effect). When the toroidal field strength reaches a critical limit, flux emergence driven by the Parker instability

¹ Department of Physics, Indian Institute of Science, Bangalore 560012, India
email: bidya_karak@physics.iisc.ernet.in

² Eötvös University, Department of Astronomy, Budapest, Hungary
email: K.Petrovay@astro.elte.hu

will give rise to active regions on the surface, with an axis tilted away from the azimuthal plane due to the Coriolis force, thereby closing the cycle (see e.g. Charbonneau, 2010 for a more detailed discussion). An attractive feature of this dynamo model is that it not only models the regular features of the solar cycle (Choudhuri, Schüssler, and Dikpati, 1995; Dikpati and Charbonneau, 1999; Chatterjee, Nandy, and Choudhuri, 2004) but also reproduces many irregular features of solar cycle (Charbonneau and Dikpati, 2000; Choudhuri and Karak, 2009; Karak, 2010; Karak and Choudhuri, 2011; Choudhuri and Karak, 2012).

In order to avoid excessive buoyant loss of toroidal flux, the Ω -effect must take place in a stably stratified layer just below the convective zone. Helioseismic inversions (Charbonneau et al., 1999; Basu and Antia, 2001) indicate that this layer coincides with the solar tachocline, i.e. the thin transitional layer between the rigidly rotating interior and the differentially rotating convective zone. The narrow radial extent of this layer (scale depth of 5–10 Mm or less) implies a strongly anisotropic angular momentum transport mechanism, much more effective in the horizontal direction than in the radial direction. Spiegel and Zahn (1992) have shown that this is possible by taking strong anisotropic turbulent viscosity in the horizontal direction. However several authors (e.g., Gough and McIntyre, 1998; Dikpati and Gilman, 1999) have found caveats in this purely hydrodynamical model and improved by including additional physics. Other most plausible candidate for such anisotropic momentum transfer is the Maxwell stress in a predominantly horizontal magnetic field configuration. One school of thought in this stream is that a weak fossil magnetic field in the radiative zone may solve this problem (Rudiger and Kitchatinov, 1997; Gough and McIntyre, 1998; MacGregor and Charbonneau, 1999). Unfortunately the simulations (Garaud, 2002; Brun and Zahn, 2006; Strugarek, Brun, and Zahn, 2011) of this so-called slow tachocline model are not able to provide uniform rotation in the radiative zone even by including penetrating flows from the convection zone, such as plumes or meridional circulation to confine the fossil magnetic field (however Garaud and Garaud, 2008 succeeded in this problem). Other school of thought is that as the dynamo generated toroidal field resides in the tachocline, it is plausible to assume that this field is responsible for the confinement of the tachocline. The feasibility of this so-called fast tachocline scenario has been demonstrated by Forgács-Dajka and Petrovay (2001, 2002) and Forgács-Dajka (2003).

In the fast tachocline scenario, the thickness of the tachocline depends on the magnetic field. This thickness, on the other hand, is one input parameter of flux transport dynamo models and thus it may be expected to influence the amplitude and configuration of the magnetic field. This coupling introduces a nonlinearity into the dynamo that may affect both the dynamo and the structure in a number of ways. Indeed, it is not a priori clear whether the fast tachocline scenario and flux transport dynamos are compatible at all, i.e. whether they can give rise to a finite amplitude oscillatory field with a tachocline of realistic thickness and with cyclic variations within the observational bounds.

The aim of the present paper is to investigate this issue. In a completely self-consistent approach one should couple the angular momentum transfer equation to the induction equation solved in dynamo models. Instead of this more generic

approach, as a first step, here we parameterize the dependence of tachocline width d_t on the poloidal field amplitude B_p with simple algebraic formulae that still retain the essential physics of the problem. Details of our problem setup are presented in Section 2. Section 3 presents the results which are then confronted with observations in Section 4. Section 5 concludes the paper.

2. Problem setup

2.1. Flux transport dynamo model

An axisymmetric magnetic field can be represented in the form

$$\mathbf{B} = B(r, \theta)\mathbf{e}_\phi + \nabla \times [A(r, \theta)\mathbf{e}_\phi], \quad (1)$$

where $B(r, \theta)$ and $A(r, \theta)$ respectively correspond to the toroidal and poloidal components. Then the evolution of magnetic fields in the flux transport dynamo model are governed by the following two equations:

$$\frac{\partial A}{\partial t} + \frac{1}{s}(\mathbf{v} \cdot \nabla)(sA) = \eta \left(\nabla^2 - \frac{1}{s^2} \right) A + S(r, \theta; B), \quad (2)$$

$$\frac{\partial B}{\partial t} + \frac{1}{r} \left[\frac{\partial}{\partial r}(rv_r B) + \frac{\partial}{\partial \theta}(v_\theta B) \right] = \eta \left(\nabla^2 - \frac{1}{s^2} \right) B + s(\mathbf{B}_p \cdot \nabla)\Omega + \frac{1}{r} \frac{d\eta}{dr} \frac{\partial(rB)}{\partial r}, \quad (3)$$

with $s = r \sin \theta$.

Here \mathbf{v} is the meridional flow which has the following analytical form.

$$v_r(r, \theta) = \frac{v_0}{f} \left(\frac{R}{r} \right)^2 \left[\frac{-1}{m+1} + \frac{c_1}{2m+1} \xi^m - \frac{c_2}{2m+p+1} \xi^{m+p} \right] \xi [2 \cos^2 \theta - \sin^2 \theta] \quad (4)$$

$$v_\theta(r, \theta) = \frac{v_0}{f} \left(\frac{R}{r} \right)^3 [-1 + c_1 \xi^m - c_2 \xi^{m+p}] \sin \theta \cos \theta, \quad (5)$$

with $\xi(r) = \frac{R}{r} - 1$, $c_1 = \frac{(2m+1)(m+p)}{(m+1)p} \xi_p^{-m}$, $c_2 = \frac{(2m+p+1)m}{(m+1)p} \xi_p^{-(m+p)}$ and $\xi_p = \frac{R}{r_p} - 1$. Here $m = 0.5$, $p = 0.25$, $v_0 = 24 \text{ m s}^{-1}$ and f is the normalization factor which determines the maximum value of the latitudinal component of the meridional circulation v_θ .

η is the turbulent magnetic diffusivity which has the following form:

$$\eta(r) = \eta_{\text{RZ}} + \frac{\eta_{\text{SCZ}}}{2} \left[1 + \operatorname{erf} \left(2 \frac{r - r_{\text{BCZ}}}{d_t} \right) \right] + \frac{\eta_{\text{surf}}}{2} \left[1 + \operatorname{erf} \left(\frac{r - r_{\text{surf}}}{d_2} \right) \right] \quad (6)$$

with $r_{\text{BCZ}} = 0.7R$, $d_t = 0.03R$, $d_2 = 0.05R$, $r_{\text{surf}} = 0.95R$, $\eta_{\text{RZ}} = 5 \times 10^8 \text{ cm}^2 \text{ s}^{-1}$, $\eta_{\text{SCZ}} = 5 \times 10^{10} \text{ cm}^2 \text{ s}^{-1}$ and $\eta_{\text{surf}} = 2 \times 10^{12} \text{ cm}^2 \text{ s}^{-1}$.

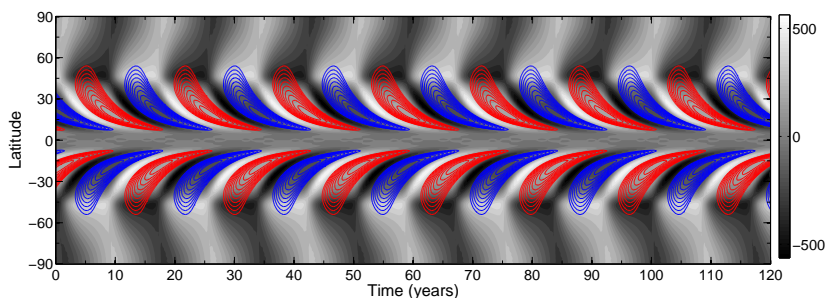


Figure 1. Reference model with fixed tachocline thickness d_t . Contours show the butterfly diagram of the toroidal field in the tachocline, the field strength being $0.91 \times 10^5 G$ at the innermost contours and half that value at the outermost contours. Blue contours correspond to positive toroidal field whereas red contours correspond to negative toroidal field. The greyscale background shows the weak diffuse radial field on the solar surface.

$S(r, \theta; B)$ is the coefficient which describes the generation of poloidal field at the solar surface from the decay of tilted bipolar sunspots (Babcock-Leighton process). It has the following form

$$S(r, \theta; B) = \frac{\alpha(r, \theta)}{1 + (B(r_t, \theta)/B_0)^2} B(r_t, \theta), \quad (7)$$

where $\alpha(r, \theta) = \frac{\alpha_0}{4} \left[1 + \operatorname{erf} \left(\frac{r-r_4}{d_4} \right) \right] \left[1 - \operatorname{erf} \left(\frac{r-r_5}{d_5} \right) \right] \sin \theta \cos \theta \left[\frac{1}{1+e^{-\gamma(\theta-\pi/4)}} \right]$ with $r_4 = 0.95R$, $r_5 = R$, $d_4 = 0.05R$, $d_5 = 0.01R$, $\gamma = 30$, $\alpha_0 = 1.6 \text{ cm s}^{-1}$ and $B_0 = 4 \times 10^4 G$.

Ω is the solar rotation which has the following form

$$\Omega(r, \theta) = \Omega_{\text{RZ}} + \frac{1}{2} \left[1 + \operatorname{erf} \left(2 \frac{r-r_t}{d_t} \right) \right] [\Omega_{\text{SCZ}}(\theta) - \Omega_{\text{RZ}}], \quad (8)$$

where r_t (the position of the tachocline) $= 0.7R$, d_t (the thickness of the tachocline) $= 0.03R$, $\Omega_{\text{RZ}}/2\pi = 432.8 \text{ nHz}$, $\Omega_{\text{SCZ}}(\theta) = \Omega_{\text{EQ}} + \alpha_2 \cos^2(\theta) + \alpha_4 \cos^4(\theta)$, with $\Omega_{\text{EQ}}/2\pi = 460.7 \text{ nHz}$, $\alpha_2/2\pi = -62.69 \text{ nHz}$ and $\alpha_4/2\pi = -67.13 \text{ nHz}$.

With the appropriate boundary conditions we solve Equations (2) and (3) in a full sphere of the meridional plane with $0.55R < r < R$, $0 < \theta < \pi$ to study the evolution of magnetic fields (see Chatterjee, Nandy, and Choudhuri, 2004 for details).

Once the transient state is over the butterfly diagram looks like the one shown in Figure 1. In this figure the contours show the toroidal field in the tachocline and the shaded background shows the strength of the radial field on the solar surface.

In the next section, we shall discuss the dependence of the tachocline thickness on the magnetic field based on the fast tachocline model and then we shall study its effect on this flux transport dynamo model.

2.2. Tachocline depth parametrization

Tachocline thickness is introduced in various ways by various authors, so care must be taken when comparing results from different papers. For a comparison it is useful to define the *relative residual angular velocity* $\tilde{\Omega}$ as

$$\tilde{\Omega}(r, \theta) = \frac{\Omega(r, \theta) - \Omega_{\text{RZ}}}{\Omega_{\text{SCZ}}(\theta) - \Omega_{\text{RZ}}}. \quad (9)$$

Clearly, $\tilde{\Omega}$ takes the value 0 in the radiative zone, 1 at the top of the tachocline. The radius r_t of the tachocline is defined by $\tilde{\Omega}(r_t, \theta) = 0.5$.

If $\tilde{\Omega}$ varies by a factor F in the radius range $[r_t - x/2, r_t + x/2]$, then clearly $x/H = \ln F$ where H is the scale height of the tachocline. From Equation (8) it then follows that our tachocline thickness parameter $d_t = 1.65H$. Similarly, for the tachocline thickness parameter w used by Antia and Basu (2011) in their helioseismic study of tachocline properties we find $w = 0.39H$, i.e. $d_t \simeq 4.3w$. This relation must be taken into account when comparing our results to observational constraints.

An approximate analytic formula relating the mean tachocline scale height H to the amplitude of an imposed poloidal field in a periodic shear layer was derived by Forgács-Dajka and Petrovay (2001). It reads

$$V_p^2 = \frac{\text{Pr} \eta r_t^2 \omega}{H^2} \frac{(1 + \eta/\omega H^2)(1 + \text{Pr} \eta/\omega H^2)}{1 + 2\text{Pr} \eta/\omega H^2}, \quad (10)$$

where $\omega = 2\pi/22$ years is the dynamo frequency, Pr is the Prandtl number, η is the turbulent magnetic diffusivity, r_t is the radius of the tachocline and V_p is the amplitude of the oscillatory poloidal magnetic field in Alfvénic units. In a turbulent medium the effective Prandtl number is expected to be order of unity, while its exact value is unknown. Therefore, in what follows we shall simply substitute d_t for H in Equation (10), ignoring the factor 1.65 between these scales as an appropriate choice of Pr can always offset this factor anyway.

Figure 2 presents the variation of B_p ($= V_p(4\pi\rho)^{1/2}$ with $\rho = 0.1 \text{ g/cm}^3$) based on the relation (10) for three different values of the diffusivity. Green curves are simpler analytical fits to each curve with a function of the form $B_p = C\eta/d_t^2$ or

$$d_t^2 = \frac{C\eta}{B_p}, \quad (11)$$

where $C = 6 \times 10^{10} \text{ G}\cdot\text{s}$, and $B_p = \sqrt{(B_r^2 + B_\theta^2)}$.

In a first attempt to relate tachocline thickness to the dynamo field by a simple power law formula, in Section 3.1 we shall employ formula (11) as a guidance in our choice of the exponent. It should be emphasized that, as Equation (11) refers to cycle averaged quantities, it should not be viewed as rigorous derivation of our coupling formulae (21) and (25)). Rather, it provides a distant analogy guiding us in our choice of a physically motivated exponent value. In particular, in the fast tachocline scenario the tachocline is confined by the Maxwell stress $B_p B$ which also involves the toroidal field strength B . The reason why B does

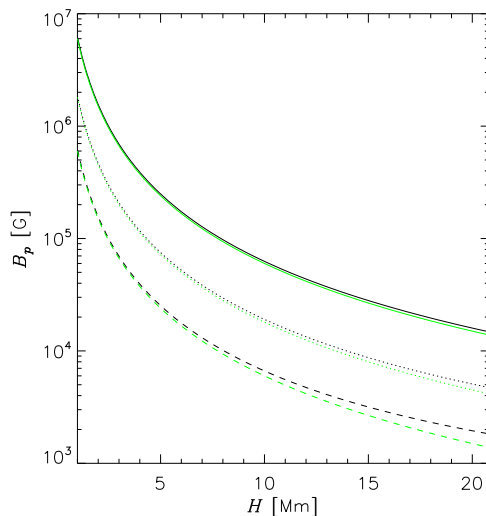


Figure 2. Relation between tachocline width d_t and poloidal field amplitude B_p for three different values of magnetic diffusivity, $\eta = 10^{12}$ (solid), $\eta = 3 \times 10^{11}$ (dotted), $\eta = 10^{11}$ (dashed). Green curves show the function $B_p = 6 \times 10^{10} \eta / d_t^2$.

not explicitly appear in Equation (11) is that the toroidal field is generated by the windup of the poloidal field, so its *overall* amplitude is ultimately determined by B_p . However, this is clearly only true for the overall amplitudes and not for the actual values of B_p and B at any given point and instant: so the simple approximate relationship (11) is, strictly speaking, only valid for the (latitudinal and temporal) average field amplitude and average tachocline thickness and its application to relate d_t and B_p at any given point in space and time is not well justified.

For this reason, in Section 3.2 we shall try to further improve on the model by relating d_t directly to the Maxwell stress. We recall from Forgács-Dajka and Petrovay (2001) that the simple model giving rise to Equation (11) consists of a semi-infinite layer bounded from above at depth $z = 0$ (“bottom of the convective zone”) where a periodic shear flow is imposed in the y direction:

$$v_{y0} = v_0 \cos(kx). \quad (12)$$

An oscillatory horizontal “poloidal” field is prescribed in the x direction throughout the volume as

$$B_x = B_p \cos(\omega t). \quad (13)$$

Introducing $v = v_y$ and using Alfvén speed units for the magnetic field

$$V_p = B_p (4\pi\rho)^{-1/2} \quad b = B_y (4\pi\rho)^{-1/2}, \quad (14)$$

the azimuthal component of the equation of motion reads

$$\partial_t v = V_p \cos(\omega t) \partial_x b - \nu \nabla^2 v, \quad (15)$$

where ν denotes viscosity. Solutions may be sought in the form

$$v = \bar{v}(x, z) + v'(x, z)f(\omega t), \quad b = b'(x, z)f(\omega t + \phi), \quad (16)$$

where f is a 2π -periodic function of zero mean and of amplitude $\mathcal{O}(1)$. (\bar{a} denotes time average of a , while $a' \equiv a - \bar{a}$.) The (temporal) average of Equation (15) then reads

$$0 = \overline{V_p \cos(\omega t) f(\omega t + \phi)} \partial_x b' - \nu \nabla^2 \bar{v}. \quad (17)$$

For an order of magnitude estimate of the terms of this equation, we assume $\overline{\cos(\omega t) f(\omega t + \phi)} \in \mathcal{O}(1)$ (i.e. no ‘‘conspiracy’’ between the phases, a rather natural assumption). As $H \ll R$ we may approximate $\nabla^2 \sim H^{-2}$. Estimating the other derivatives as $\partial_t \sim \omega$ and $\partial_x \sim R^{-1}$, (17) yields

$$V_p b' / R \sim \nu \bar{v} / H^2, \quad (18)$$

i.e.,

$$H^2 \simeq \frac{\nu R \bar{v}}{V_p b'} \quad (19)$$

or, switching back to conventional magnetic field units and from H to d_t :

$$d_t^2 = \frac{C' \eta}{B_p B}. \quad (20)$$

Plugging in the correct dimensional values we find $C' \simeq 2 \times 10^{15} \text{ G}^2 \cdot \text{s}$ —this is the value we use in Section 3.2 below where, again, we shall employ formula (20) as a guidance in our choice of the exponent of our simple feedback formula. While the link between tachocline thickness and Maxwell stress is more direct than between d_t and B_p alone, it should still be kept in mind that equation (20) refers to cycle averaged quantities, so it should not be viewed as a rigorous derivation of our coupling formulae (26) and (29). Rather, it provides an analogy guiding us in our choice of a physically motivated exponent value.

3. Results

3.1. Tachocline thickness linked to poloidal field amplitude

In the fast tachocline scenario the thickness of the tachocline may vary as a function of both time and latitude. For a fully consistent treatment of this variation the equation of motion should be coupled to the dynamo equations. However, in the present preliminary exploration of the problem we are only interested in the general stability properties and robustness of flux transport dynamo against the kind of nonlinearity introduced by the fast tachocline mechanism. Therefore, we

simplify the problem by an appropriate parametrization of the dependence of d_t on the magnetic field. For this purpose any arbitrary numerical relation between tachocline thickness and magnetic field may do as long as it results in d_t values of the right order of magnitude and it has the expected property of resulting in a thinner tachocline for stronger magnetic fields.

The numerical relation we first consider here is Equation (11). As we already remarked in Section 2.2, by its derivation, the formula (11) given above only relates the cycle and latitude averaged mean value of the tachocline thickness to the amplitude of the variation of the poloidal field, and our use of it to link local and momentary values of these variables is arbitrary. Nevertheless, by its construction, Equation (11) does have the required properties of resulting in d_t values of the right order of magnitude and in a thinner tachocline for stronger magnetic fields, so it will suffice for the purpose of a first exploration.

For a first study we shall not consider any latitudinal variation of the tachocline. Substituting the appropriate turbulent value for η in the tachocline we then have

$$d_t^2 = \frac{C\eta_t}{B_p(t)} \quad (21)$$

where

$$\eta_t = \frac{1}{2d_0} \int_{r_t-d_0}^{r_t+d_0} \eta(r) dr \quad (22)$$

with $d_0 = 0.015R$.

$$\bar{B}_p(t) = \frac{2}{\pi} \int_0^{\pi/2} \bar{B}_p(\theta, t) d\theta \quad (23)$$

is the latitude averaged poloidal field amplitude while $\bar{B}_p(\theta, t)$ is the local radial mean value of the poloidal field calculated as

$$\bar{B}_p(\theta, t) = \frac{1}{2d_0} \int_{r_t-d_0}^{r_t+d_0} \bar{B}_p(r, \theta, t) dr. \quad (24)$$

(Recall that $\bar{B}_p = \sqrt{(B_r^2 + B_\theta^2)}$, i.e. the modulus of the poloidal field. This ensures that \bar{B}_p , as given in the above equations, remains positive at all times.)

Now, starting from the relaxed state of our (fixed d_t) model discussed in Section 2.1, we allow d_t to vary at every time step of our simulation, calculating $\bar{B}_p(t)$ as above to get the value of d_t from Equation (21). The calculation is run again for several solar cycles until it relaxes to a nearly steady cyclic behavior. In Figure 3, we show a few solar cycles long clip just after this modification. It is noteworthy that this kind of tachocline structure calculated from the fast tachocline model does produce a periodic solar-like solution. In the upper panel, the butterfly diagram of toroidal and radial field components is shown. The appearance of this plot is quite similar to the one found in Figure 1 in Section 2.1. Therefore we may conclude that the fast tachocline model and the flux transport dynamo model are compatible and a nonlinear coupling between tachocline thickness and field amplitude does not lead to a breakdown of the solar-like solution.

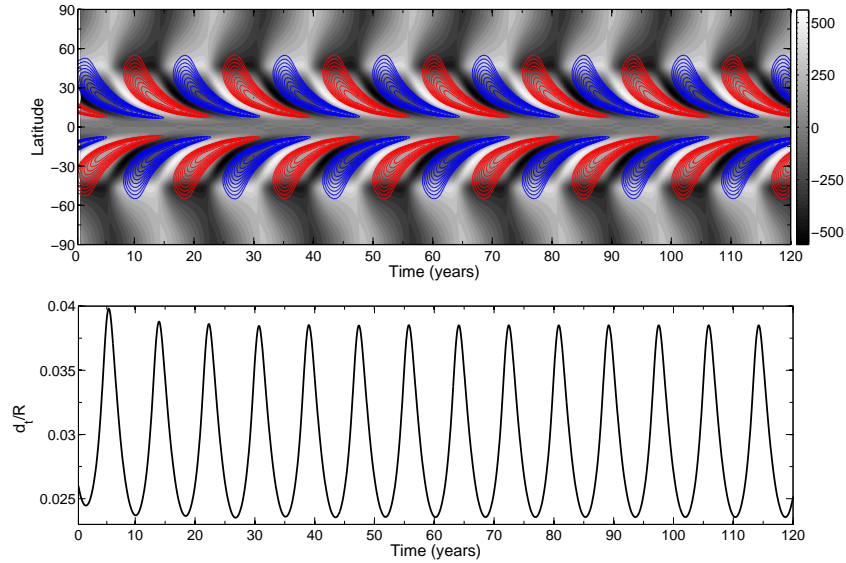


Figure 3. Upper panel: same as Figure 1 but for variable tachocline thickness d_t as given by eq. (21). Lower panel: variation of tachocline thickness d_t with time.

The lower panel shows the variation of d_t with solar cycle. The amplitude of this variation is about $\pm 25\%$.

Next, we try to explore the latitudinal structure of the tachocline by admitting d_t to depend on θ , i.e. instead of Equation (21) we use

$$d_t^2 = \frac{C\eta_t}{\overline{B}_p(\theta, t)}. \quad (25)$$

Figure 4 presents the result for this calculation. Upper panel shows the butterfly diagram which still resembles most characteristics of the observed butterfly diagram.

3.2. Tachocline thickness linked to the Maxwell stress

In our next parametric study we link the tachocline thickness d_t to the Maxwell stress by formula (20). Again, for our first study we disregard the latitude dependence in d_t :

$$d_t^2 = \frac{C'\eta_t}{\overline{B}_p(t)\overline{B}(t)} \quad (26)$$

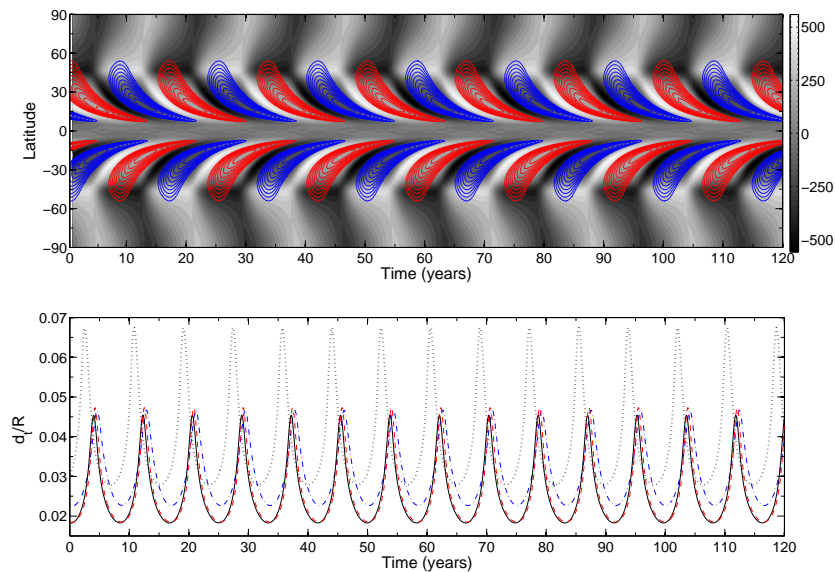


Figure 4. Upper panel: same as Figure 1 but for variable tachocline thickness d_t as given by eq. (25). Lower panel: variation of tachocline thickness d_t with time at different latitudes. Dash-dotted, solid, dashed and dotted lines are the values at 75° , 60° , 45° and 15° latitudes, respectively.

The mean values of B are here defined in a manner analogous to those of B_p :

$$\bar{B}(t) = \frac{2}{\pi} \int_0^{\pi/2} \bar{B}(\theta, t) d\theta \quad (27)$$

is the latitude averaged toroidal field amplitude while $\bar{B}(\theta, t)$ is the local radial mean value of the toroidal field calculated as

$$\bar{B}(\theta, t) = \frac{1}{2d_0} \int_{r_t-d_0}^{r_t+d_0} |B(r, \theta, t)| dr. \quad (28)$$

(Again, using the modulus of the toroidal field in the integrand ensures that \bar{B} , as given in the above equations, remains positive at all times.)

The result is shown in Figure 5.

Finally, to explore the latitude dependence of tachocline thickness we set

$$d_t^2 = \frac{C' \eta_t}{\bar{B}_p(\theta, t) \bar{B}(\theta, t)}. \quad (29)$$

This yields what we may regard our most realistic model. Figure 6 shows the result.

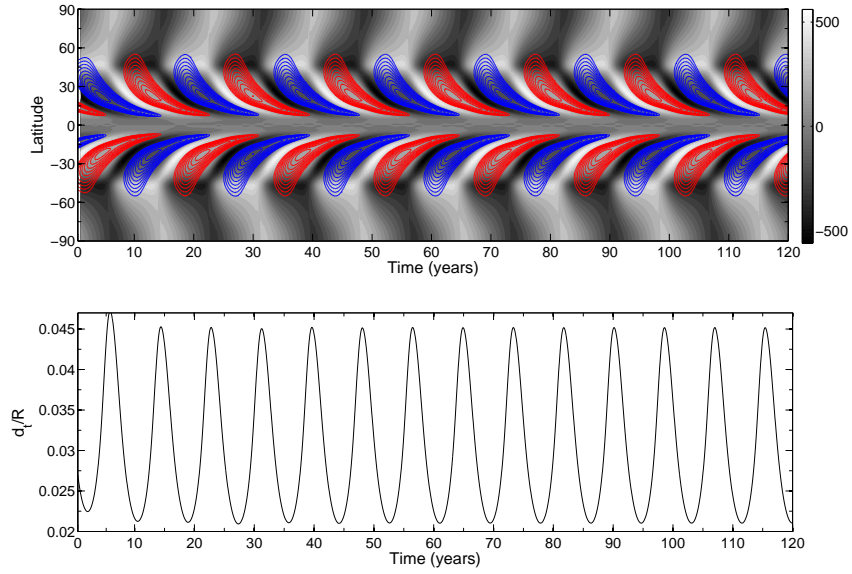


Figure 5. Same as Figure 3 but here the tachocline thickness d_t is determined by eq. (26).

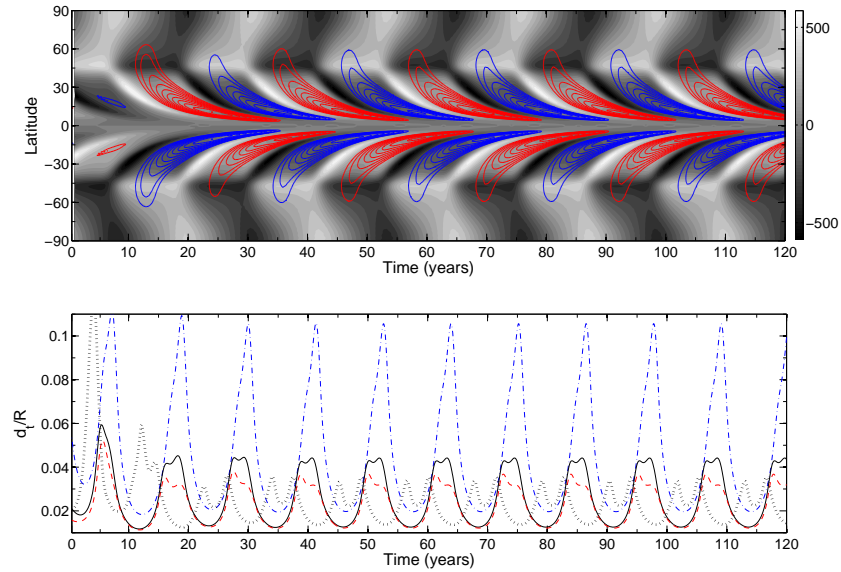


Figure 6. Same as Figure 4 but here the tachocline thickness d_t is determined by eq. (29) (most realistic model). In the lower panel, the dash-dotted, solid, dashed and dotted lines are the values of d_t at 75° , 60° , 45° and 15° latitudes, respectively.

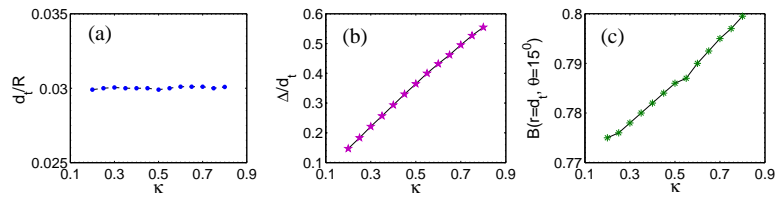


Figure 7. Variation of tachocline thickness d_t (a); of the amplitude variation of the tachocline thickness Δ/d_t (b); and of toroidal field strength at 15° latitude (c) as functions of κ (the exponent in Equation 30).

4. Discussion

The properties of the variable tachocline resulting from our models may be compared to empirical (helioseismic) constraints. An in-depth study of tachocline thickness as a function of latitude and time was recently performed by Antia and Basu (2011) (also see Basu and Antia, 2001). Converting their tachocline thickness parameter w to our parameter d_t as discussed in Section 2.2 above, their finding was that d_t/R varies from approximately 0.02 to 0.1 with increasing heliographic latitude. Temporal variations of up to $\pm 50\%$ are observed; however these are dominated by variation on the time scale of a few years. (Variations on such time scales may be produced by shear instabilities, cf. Miesch, 2007) On the longer time scale of 11 years no systematic variations were detected; from visual inspection of the relevant figures, this sets an upper limit of $\sim \pm 20\%$ on cycle related changes in tachocline thickness.

The mean value of tachocline thickness in Figures 3–6 lies around $0.03R$. In the most realistic case, Figure 6, the thickness varies from 0.02 to 0.1 as we move from low to high latitudes, in perfect agreement with the observations. This demonstrates that the simple analytical feedback formula (29) not only gives a solar like dynamo solution in the flux transport dynamo model but also reproduces the realistic value *and* the observed latitude dependence of the tachocline thickness.

The cycle variation of tachocline thickness found in our models is quite significant, up to $\pm 30\%$. This is somewhat higher than what the observational constraints suggest.

In order to explore how sensitive our quantitative results are to details of the feedback formula, we generalize Equation (29) as

$$d_t = \frac{(C'\eta_t)^{1/2}}{[B_p(\theta, t)B(\theta, t)]^\kappa}. \quad (30)$$

Clearly, the case $\kappa = 0.5$ returns Equation (20). While using other values of κ has no clear physical justification, it offers a way to explore the sensitivity of our quantitative results to details of the feedback formula chosen.

We repeat the same calculation at different values of κ ranging from 2 to 8. Figure 7 presents the results. Panel (a) shows the variation of d_t as a function of κ . Note that as we vary κ , we also vary C' in order to fix the mean value of

d_t at around $0.03R$ which is fairly close to the observed value. (As C' involves the unknown quantity Pr , its value is not well constrained anyway.) Figure 7(b) shows the amplitude Δ of the departure of d_t from its mean value as a function of κ . A smooth increase with κ is found, so lower κ values result in rather more subdued thickness variations that may be compatible with more stringent empirical limits. Following Choudhuri (2003) we should keep in mind that as we are using mean field dynamo equations, the Maxwell's stress $B_p B$ is consist of the mean values of B_p and B and thereby these are non-zero only inside the flux tubes. Now if $(B_p)_{\text{ft}}$ and $(B)_{\text{ft}}$ are the values of these quantities inside flux tubes and f is the filling factor, then we have $B_p = f(B_p)_{\text{ft}}$ and $B = f(B)_{\text{ft}}$ (we assumed the same filling factor for both components for the sake of simplicity). Therefore it is easy to show that the mean stress appeared in all the calculations of Section 3.2 should be replaced by the $f(B_p)_{\text{ft}} (B)_{\text{ft}} = B_p B / f$. However this factor f can be absorbed in the C' because C' is not a strict constant.

5. Conclusion

We have explored the compatibility of the fast tachocline model with the flux transport dynamo model. For this purpose we employed two simple feedback formula, Equations (25) and (29), relating the thickness of the tachocline to the poloidal magnetic field strength. While the second of these formulae is physically more sound, both reflect the expected form of the relationship between cycle averaged tachocline thickness and the amplitude of the magnetic field, and they do have the required properties of resulting in d_t values of the right order of magnitude and in a thinner tachocline for stronger magnetic fields. Both cases were studied with and without latitude dependence in d_t .

The flux transport dynamo model we considered proved to be robust against the nonlinearity introduced by this simplified fast tachocline mechanism. Solar-like butterfly diagrams were found to persist and the overall thickness of the tachocline is well within the range admitted by helioseismic constraints even without any parameter fitting. In the most realistic case of a time and latitude dependent tachocline thickness linked to the value of the Maxwell stress, d_t and its latitude dependence are in excellent agreement with seismic results.

One characteristic of fast dynamo mechanism is a marked cycle dependence in tachocline properties. Indeed, without parameter fitting, in all of our models the cycle related changes in tachocline thickness are somewhat larger than the maximal such variation admitted by helioseismic constraints. On the other hand, an exploration of the parameter space indicates that in a slightly generalized form of our feedback formula it is possible to find parameter combinations where the cycle variation remains within the observational bounds while in other respects the good agreement of our model with observations is preserved.

While there is no straightforward physical justification for such a generalized feedback formula, our parametric study shows that results like the compatibility of the fast dynamo and flux transport dynamo mechanism, the overall thickness of the tachocline or the amplitude of the toroidal field are more robust than details like the time and latitude dependence. Physical effects not considered

in our model may, then, potentially be held responsible for the deviation of the feedback formula exponent from the value of 0.5 derived from a simplified analytic model.

Such further effects may include tachocline instabilities, a change in the geometric setup of our dynamo model or a combination of the two. One clear limitation of the model is that differential rotation is quite strong at high latitudes, so one may expect that this is the region where strong toroidal field is produced. However, sunspots appear at low latitudes only. In the Surya family of models on which our model is based, this problem is bypassed by considering a deeply penetrating meridional flow (Nandy and Choudhuri, 2002). While this may be unphysical, it has the desired effect of allowing the toroidal field generated at higher latitudes to be stored and amplified further until it reaches the lower latitudes where sunspot eruptions happen. A promising, and more physically consistent way out of this conundrum was suggested by Parfrey and Menou (2007) who showed that at latitudes higher than 37° the magnetorotational instability (MRI) is present in the tachocline, presumably resulting in stronger turbulence, a thicker tachocline and a less organized field structure. All this just serves to illustrate that, independently of the choice of our feedback formula, there may be more physical effects to consider before we can hope to simultaneously reproduce the correct temporal and latitudinal structure of the tachocline.

A further obvious limitation is that only one particular dynamo model was considered. It is well known that properties of flux transport dynamos are quite sensitive to variations in the input parameters and assumptions (e.g. Dikpati et al., 2002; Guerrero and de Gouveia Dal Pino, 2007; Jiang, Chatterjee, and Choudhuri, 2007; Yeates, Nandy, and Mackay, 2008; Karak and Choudhuri, 2012; Karak and Nandy, 2012). It is therefore desirable to extend such studies to other dynamo configurations.

It is nevertheless clear that the use of simple feedback formulae of any form via a simplified approach to the problem can only be considered as a first exploration. In any case, the completely consistent treatment of the problem should involve the full solution of the equation of motion, coupled with the dynamo equations.

Acknowledgements We thank Prof. Arnab Rai Choudhuri for raising valuable points which certainly improved this paper. For our dynamo calculations we have used Surya code developed in Choudhuri's group at Bangalore. Support by the Hungarian Science Research Fund (OTKA grants no. K83133 and 81421) and by the European Union with the co-financing of the European Social Fund (grant no. TÁMOP-4.2.1/B- 09/1/KMR-2010-0003) is gratefully acknowledged. BBK thanks CSIR, India for financial support and also to ELTE for comfortable hospitality during the beginning of this work.

References

- Antia, H.M., Basu, S.: 2011, *Astrophys. J. Lett.* **735**, L45.
 Brun, A.S., Zahn, J.-P.: 2006, *Astron. Astrophys.* **457**, 665.
 Basu, S., Antia, H.M.: 2001, *Mon. Not. Roy. Astron. Soc.* **324**, 498.
 Charbonneau, P.: 2010, *Living Rev. Solar Phys.* **7**, 3.

- Charbonneau, P., Dikpati, M.: 2000, *Astrophys. J.* **543**, 1027.
- Charbonneau, P. Christensen-Dalsgaard, J., Henning, R., Larsen, R.M., Schou, J., Thompson, M.J. et al.: 1999, *Astrophys. J.* **527**, 445.
- Chatterjee, P., Nandy, D., Choudhuri, A.R.: 2004, *Astron. Astrophys.* **427**, 1019.
- Choudhuri, A.R.: 2003, *Solar Phys.* **215**, 31.
- Choudhuri, A.R., Karak, B.B.: 2009, *Res. Astron. Astrophys.* **9**, 953.
- Choudhuri, A.R., Karak, B.B.: 2012, *Phys. Rev. Lett.* submitted (arXiv:1208.3947).
- Choudhuri, A.R., Schüssler, M. Dikpati, M.: 1995, *Astron. Astrophys. Lett.* **303**, L32.
- Dikpati, M., Charbonneau, P.: 1999, *Astrophys. J.* **518**, 508.
- Dikpati, M., Gilman, P.A.: 1999, *Astrophys. J.* **512**, 417.
- Dikpati, M., Corbard, T., Thompson, M.J., Gilman, P.A.: 2002, *Astrophys. J. Lett.* **575**, L41.
- Forgács-Dajka, E., Petrovay, K.: 2001, *Solar Phys.* **203**, 195.
- Forgács-Dajka, E., Petrovay, K.: 2002, *Astron. Astrophys.* **389**, 629.
- Forgács-Dajka, E.: 2003, *Astron. Astrophys.* **413**, 1143.
- Garaud, P.: 2002, *Mon. Not. Roy. Astron. Soc.* **329**, 1.
- Garaud, P., Garaud, J.-D.: 2008, *Mon. Not. Roy. Astron. Soc.* **391**, 1239.
- Gough, D.O., McIntyre, M.E.: 1998, *Nature* **394**, 755.
- Guerrero, G., de Gouveia Dal Pino, E. M.: 2007, *Astron. Astrophys.* **464**, 341.
- Jiang, J., Chatterjee, P., Choudhuri, A.R.: 2007, *Mon. Not. Roy. Astron. Soc.* **381**, 1527.
- Karak, B.B.: 2010, *Astrophys. J.* **724**, 1021.
- Karak, B.B., Choudhuri, A.R.: 2011, *Mon. Not. Roy. Astron. Soc.* **410**, 1503.
- Karak, B.B., Choudhuri, A.R.: 2012, *Solar Phys.*, **278**, 137.
- Karak, B.B., Nandy, D.: 2012, arXiv:1206.2106.
- MacGregor, K.B., Charbonneau, P.: 1999, *Astrophys. J.* **519**, 911.
- Miesch, M.S.: 2007, *Astrophys. J. Lett.* **658**, L131.
- Nandy, D., Choudhuri, A.R.: 2002, *Science* **296**, 1671.
- Parfrey, K.P., Menou, K.: 2007, *Astrophys. J. Lett.* **667**, L207.
- Rudiger, G., Kitchatinov, L.L.: 1997, *Astron. Nachr.* **318**, 273.
- Spiegel, E.A., Zahn, J.-P.: 1992, *Astron. Astrophys.* **265**, 106.
- Strugarek, A., Brun, A.S., Zahn, J.-P.: 2011, *Astron. Astrophys.* **532**, 34.
- Yeates, A.R., Nandy, D., Mackay, D.H.: 2008, *Astrophys. J.* **673**, 544.